Molecular Phylogenetics and Evolution 224 (2026) 108674

Contents lists available at ScienceDirect

Molecular Phylogenetics and Evolution

journal homepage: www.elsevier.com/locate/ympev

Resolving fuzzy species limits: nuclear evidence for speciation by hybridisation in Amazonian *Trichomanes* ferns

Laura Kragh Frederiksen [a,*], Jami Sundström [b], Wolf L. Eiserhardt [a,c], Hanna Tuomisto [a,b]

[a] Department of Biology, Aarhus University, 8000 Aarhus C, Denmark
[b] Department of Biology, University of Turku, 20014 Turku, Finland
[c] Royal Botanic Gardens, Kew, Richmond, Surrey TW9 3AE, United Kingdom

ARTICLE INFO

Keywords:
Ferns
GoFlag
HybPhaser
Hybridisation
Neotropics
Nuclear genes
Speciation

ABSTRACT

Unclear species boundaries are a common challenge in ecological studies and species inventories, obscuring patterns of biodiversity and complicating inferences about ecological and evolutionary processes. One possible cause of fuzziness is hybridisation, but little information exists on hybridisation in the tropics. Here we aim to address the question of potential hybridisation in the tropical American fern genus *Trichomanes* (Hymenophyllaceae) and to clarify evolutionary relationships within the genus. We take advantage of nuclear target-capture sequencing, haplotype phasing and off-target plastid reads to detect phylogenetic relationships and reticulate histories. We sampled 303 individuals that represent 41 known *Trichomanes* species. Our analyses recovered a robust backbone for the genus, strongly supporting subgenus *Trichomanes* as sister to subgen. *Feea*, and subgen. *Davalliopsis* as sister to subgen. *Lacostea*. *Trichomanes pinnatum* proved to be a complex where six different unnamed morphs represent four different kinds of evolutionary history. Two morphs appear to be stabilised, relatively old hybrid-derived species, one represents a recent hybrid, one reflects repeated spontaneous hybridisation between the same parent species, and one represents within-species morphological variation without any obvious genomic signal. Excluding the four hybrids makes *T. pinnatum* s.s. morphologically and genetically much more uniform, but its geographic distribution still covers practically all tropical America, indicating that the species may be approaching panmixia.

1. Introduction

Ecological studies and species inventories often struggle with diffusely varying morphological similarity, which makes it difficult to decide if the observed individuals represent the same species or more than one closely related species (Bickford et al., 2007; Hending, 2025). Understanding such cryptic diversity has direct implications for measuring biological diversity, inferring evolutionary processes, understanding the functioning of ecosystems, and prioritising conservation efforts (González-Orozco and Parra-Quijano, 2023; Mace, 2004; Rojas, 1992). For example, widespread and common taxa are generally of less conservation concern than species with smaller populations and more restricted geographical ranges (Funk et al., 2012). Species delimitation is especially challenging in tropical rainforests, where extraordinary species richness is combined with relatively low level of taxonomic attention (Balakrishnan, 2005; Dexter et al., 2010; Freeman and Pennell, 2021; Ruokolainen et al., 2002).

The availability of molecular methods has helped solve many taxonomical problems, and often what was thought to be one morphologically variable species has been revealed to consist of a complex of two or more independent species that may be more restricted in their environmental and/or biogeographical distributions (Janzen et al., 2017). Integrating morphology, molecular data, and distributional and ecological information can provide a powerful route to resolve species limits, recognise novel taxa and test for evolutionary relationships in morphologically complex groups (Maltsev and Erst, 2023). This has recently been seen in Amazonia and other tropical American rainforests, where extensive field work has suggested that many widespread species may be species complexes. There are several examples of such complexes having been resolved in revisions using integrative taxonomy both in ferns (*Metaxya* by Cárdenas et al. (2016); *Salpichlaena* by Cárdenas et al. (2019); *Danaea* by Keskiniva et al. (2024)) and in

* Corresponding author.
E-mail address: laura.frederiksen@bio.au.dk (L.K. Frederiksen).

https://doi.org/10.1016/j.ympev.2026.108674
Received 8 March 2026; Received in revised form 23 June 2026; Accepted 27 June 2026
Available online 3 July 2026

angiosperms (*Cycnoches* by Pérez-Escobar et al. (2017); *Miconia* by Goldenberg et al. (2013); *Inga* by Nicholls et al. (2015)).

Among the conspicuous remaining problem cases is the *Trichomanes pinnatum* complex (Hymenophyllaceae; we follow the nomenclature of Hassler (2026)). This is a terrestrial fern that is widespread and relatively common across tropical America and is also well-known thanks to its distinctive morphology (Fig. 1). However, floristic inventories have separated from the traditional concept of *T. pinnatum* several morphs, some of which occur widely across Amazonian rainforests and appear to behave like independent species. Since matching species names have not yet been found, for the time being the morphs are identified by unique ID numbers (all unidentified species in the genus were originally given consecutive numbers, but many of the numbers are no longer in use as they have been replaced by proper names). Although their limits are somewhat fussy, each morph seems to occur in slightly different environments within the rainforest: *T.* sp1 is common in waterlogged sites and swamps, *T.* sp4 on hill tops, and *T. pinnatum* s. str. in topographically intermediate positions (HT, pers. obs.). In addition, observations have been made of a morph that has unusually long sterile leaves with many pinnae (*T.* sp11) and morphs intermediate in appearance between *T. pinnatum* and *T. hostmannianum* (*T.* sp3) or between *T. pinnatum* and *T. vittaria* (*T.* sp21). One can hypothesise that these morphs represent either independent species, hybrids between species, or phenotypic variation within a species. Since the alternative hypotheses make different predictions about the phylogenetic relationships of the morphs, they can be tested using molecular phylogenetic methods.

Trichomanes currently comprises 72 recognised species (Hassler, 2026). The genus is of general interest because it is relatively consistently present in tropical American rainforests, and since different species grow on different kinds of soils, they can be used as indicators of forest site types (Salovaara et al., 2004; Tuomisto and Poulsen, 1996). For example, two well-known representatives of subgen. *Feea* indicate contrasting soils in Amazonia: *T. diversifrons* grows on relatively nutrient-rich soils and *T. trollii* on relatively poor soils, and consequently their Amazon-wide distributions are also different (Van doninck et al., 2020). However, there are groups in *Trichomanes* within which herbarium specimens are inconsistently identified or they express morphological variation of insufficiently understood taxonomic significance.

Reticulate evolution (hybridisation and introgression) is increasingly recognised as a major driver of plant diversification, especially in ferns (Barrington et al., 1989; Bloesch et al., 2022; Keskiniva et al., 2025; Manton, 1950; Rothfels et al., 2015; Soltis and Soltis, 2009; Tseng et al., 2024). However, many fern hybrids exhibit sterility that may limit introgressive gene flow, though genomic studies have demonstrated introgression in some systems (e.g. Wang et al., 2020; Sigel, 2016).

Reticulation can also contribute to the difficulty of establishing species limits by producing intermediate morphologies and introducing conflicting signals into phylogenetic trees. Cytological observations suggest that allopolyploidy (hybridisation combined with genome doubling; Abbott et al., 2013; Soltis and Soltis, 2009) may have been common in *Trichomanes* (Abreu et al., 2024). Most species have a karyotype of $2n = 64$, but much higher counts are also known. For example, an allopolyploid ($12x$) between *T. crispum* ($2n = 8x = 256$) and

Fig. 1. Photographs of *Trichomanes* sect. *Neurophyllum* with known species on the upper row and numbered distinct-looking morphs on the lower row. (A), *T. hostmannianum*; (B), *T. pinnatum* s. str.; (C), *T. vittaria*; (D), *T.* sp1; (E), *T.* sp4; (F), *T.* sp11 and (G), *T.* sp21. Photos: (A–F) by Hanna Tuomisto; (G) by New York Botanical Garden.

T. robustum E.Fourn. ($2n = 4x = 128$) showed $2n = 384$, along with intermediate morphology and irregular meiosis (Walker, 1985). These cytological patterns indicate that hybridisation and polyploidy may have played an underappreciated role in the diversification of the genus. Both processes can contribute to making species identification more difficult, so clarifying their contribution can have practical advantages in addition to illuminating how population genomic and evolutionary processes operate.

Analysis of nuclear data is now making it possible to identify signatures of hybridisation and introgression. Hybrid genomes often show a high degree of heterozygosity and polymorphism (Nauheimer et al., 2021), and haplotype phasing allows splitting DNA reads into maternal and paternal haplotypes. Treating the two separately helps both to reduce conflicting signals in phylogenetic analyses and to identify parentage (Bloesch et al., 2022; Keskiniva et al., 2025; Pelosi et al., 2024; Tseng et al., 2024). Phylogenetic studies on *Trichomanes* have so far relied entirely on a few plastid markers (Dubuisson et al., 2022, 2003; Ebihara et al., 2007; Lehtonen, 2011; Nitta et al., 2022), which are always maternally inherited and therefore, on their own, unable to reveal reticulate evolution.

Here we sampled 303 individuals representing 41 known *Trichomanes* species and eight unnamed morphs, five of which were within the *T. pinnatum* complex and three in subgenus *Davalliopsis*. We used nuclear target capture to (1) reassess evolutionary relationships within *Trichomanes*, (2) test for possible hybridisation within the genus, (3) evaluate phylogenetic patterns within the *T. pinnatum* complex in the context of its high morphological variability, and (4) assess current species circumscriptions within the genus to inform a forthcoming taxonomic revision. The results will contribute to a more robust framework for biodiversity assessments and for understanding the diversification, biogeography, and trait evolution in tropical ferns.

2. Materials and methods

2.1. Taxon sampling and DNA sequencing

We focused on tropical American *Trichomanes* and aimed for broad sampling, including multiple specimens per species from different parts of their range where possible (Supplementary Table S1). Silica-dried samples were obtained both through own field work and from colleagues, with the appropriate permits having been obtained prior to field work. In addition, many species were sampled from herbarium specimens with permission from the respective herbaria. The source herbarium for each sample is given in Supplementary Table S2. Most specimens also have duplicates in other herbaria, at least in the country of origin. *Abrodictyum*, *Didymoglossum* and *Vandenboschia* were used as the outgroup (Dubuisson et al., 2022). Nomenclature is according to Hassler (2026); complete species names with authors are also listed in Supplementary Table S2. Throughout the paper, we use the abbreviation sp. followed by a unique number to refer to species that have been identified as distinct in field inventories but not yet matched with a species name, and the abbreviation aff. to indicate that a specimen could be identified as the species in question based on its morphology, but our genomic data and herbarium work suggest it to be distinct.

For DNA extraction, leaf fragments (ca. 1–2 cm^2) from silica-gel dried and herbarium specimens were pulverised using a mortar and pestle with liquid nitrogen and sterile sand. DNA extraction followed the modified CTAB protocol described in Doyle and Doyle (1987). Already extracted DNA was available for several samples (see Supplementary Table S2). DNA quality was assessed using gel electrophoresis and an Agilent TapeStation (Agilent, Santa Clara, California, U.S.A.), and quantity was assessed via a Quantus fluorometer (Promega, Madison, Wisconsin, U.S.A.). DNA shearing to target size was performed when necessary, using a Covaris ME220 ultrasonicator, targeting 300–400 bp insert sizes (Covaris, Woburn, Massachusetts, U.S.A.).

Libraries were prepared with the NEBNext Ultra II DNA Library Prep Kit for Illumina (New England BioLabs Ltd, Hitchin, U.K.), using 50–200 ng of DNA input, half volumes of buffer and adapters (Hale et al., 2020), and 10–12 PCR cycles. Library quality was verified using an Agilent 4200 TapeStation. Total genomic DNA libraries were enriched for selected target loci using a custom RNA bait kit (MyBaits, Arbor Biosciences, Michigan, U.S.A.), targeting the GoFlag-408 loci (Breinholt et al., 2021). Enrichment was carried out in pools of 3–22 libraries, following manufacturer's protocols. Enriched libraries were sequenced on an Illumina NovaSeq X Plus Series (PE150; Illumina, San Diego, California, U.S.A.).

2.2. Nuclear data

2.2.1. Trimming and sequence assembly

Sequence reads were trimmed for Illumina adapters and low-quality bases using Trimmomatic v0.39 (Bolger et al., 2014; parameters: illuminaclip 1:30:7:1, leading 30, slidingwindow 4:30, minlen 40). Read quality was assessed pre- and post-trimming with FastQC v0.11.9 (Andrews, 2010) and summarised using MultiQC v1.13 (Ewels et al., 2016). Trimmed reads were assembled using HybPiper v2.0.1rc (Johnson et al., 2016) using BWA v0.7.17 (Li and Durbin, 2009). For practical reasons, we used a reference file for all 451 loci described by Breinholt et al. (2021), i.e. including 43 loci that were not enriched in our libraries. This reference file was generated with the script '1_extractSequences.sh' (Testo, 2023) and only included the leptosporangiate-monilophyte sequences, corresponding to 436 loci. Reads matching each target locus were assembled with SPAdes v3.15.5 (Bankevich et al., 2012) using default cut-off coverage. Exons plus flanking intron and spacers (supercontigs) were retrieved for downstream analyses.

Assessing HybPiper statistics we found that the initial reference file, which included leptosporangiate-monilophyte sequences from GoFlag, resulted in very low on-target read recovery (<2%). The reported success rate has ranged from 0.1% to 89.9%, depending on organism (Breinholt et al., 2021). To improve recovery while minimising the risk of reinforcing paralogous loci, we supplemented the reference with *Trichomanes* supercontig sequences that were inferred to be single-copy based on HybPiper paralog statistics, to get a closer match between reference file and samples. We ensured coverage of all loci by selecting sequences from different *Trichomanes* samples from the first run that together had sequences for all loci. Re-running HybPiper with this updated reference file increased on-target reads to 1.3–90.1% (Supplementary Table S3). Although this approach introduces some taxonomic bias in assembly, it reflects a deliberate trade–off between improving reference similarity and avoiding the inclusion of paralogous loci.

2.2.2. Data analyses

To remove multi-copy genes, we analysed the composition of SNPs (single nucleotide polymorphisms) across samples and loci using the HybPhaser v2.0 bioinformatic workflow (Nauheimer et al., 2021). Following default HybPhaser settings, SNPs were only mapped when coverage was at least 10x, allele frequency was at least 0.15, and the alternative allele occurred in at least four reads. Loci with unusually high SNP levels were identified as statistical outliers (i.e. exceeding 1.5 × the interquartile range above the third quartile) and removed as likely multi-copy genes following Nauheimer et al. (2021).

Additionally, samples with a proportion of recovered loci and total recovered target sequence length below 18% were filtered out. This threshold for total recovered target sequence length was selected based on removing samples with exceptionally short sequence lengths from further analyses, corresponding to the point where the curve begins to stagnate in a plot showing the $\log_{10}$ transformed sequence lengths of all loci (Supplementary Fig. S1). The same 18% threshold was also applied to the proportion of recovered loci, but this criterion did not result in the exclusion of any additional samples.

Consensus sequences for the samples remaining after filtering were aligned individually for each gene using the G-INS-i algorithm and "adjustdirection" options of MAFFT v7.508 (Katoh and Standley, 2013). Fragmentary sites with high proportions of missing data were removed with trimAL v1.4.1 (Capella-Gutiérrez et al., 2009) for gap thresholds (gt) ranging from 0.1 to 0.95 in increments of 0.05. The 'optrimAL' R script of Shee et al. (2020) was then applied to set the optimal trimming threshold for each gene, based on AMAS v1.0 (Borowiec, 2016) summary statistics. We further refined the alignments using CIalign v1.0.18 (Tumescheit et al., 2022) to remove noise, such as cropping poorly aligned ends and TAPER (Zhang et al., 2021) to mask errors in small, species-specific areas in the alignment.

Gene trees were inferred with IQ-TREE v2.2.0.3 (Minh et al., 2020) using maximum likelihood and 1000 ultrafast bootstrap replicates (Hoang et al., 2018), and the best-fit substitution model selected using ModelFinder (Kalyaanamoorthy et al., 2017). A species tree was inferred from the gene trees using the quartet-based method ASTRAL-hybrid in ASTER v1.16, which reduces the impact of quartets with low support and/or long terminal branches (Zhang and Mirarab, 2022), rooting the tree on the species *Vandenboschia collariata*.

2.3. Plastid data

2.3.1. Retrieval, inclusion criteria and phylogenetic analysis

To recover plastid sequences from off-target reads, we used the 'cpDNA' pipeline (Leempoel and Bailey, 2025) with minor modifications. Raw nuclear sequencing data, trimmed only for adapters using Trimmomatic, were used as input. Plastid genomes were assembled from these reads using GetOrganelle 1.7.5 (Jin et al., 2020) with recommended parameters (i.e. −R 20 −k 21, 45, 65, 85, 105).

To extract individual plastid regions, the assemblies were mapped against a reference set of plastid genes using BLASTN (Camacho et al., 2009). The reference consisted of the fully annotated plastome of *Trichomanes trollii* (NCBI accession, https://www.ncbi.nlm.nih.gov/nuccore/NC_041122.1), currently the only complete plastome available for the genus (Lehtonen, 2018). The plastid dataset included all samples from the nuclear dataset that recovered at least one of the 124 plastid loci present in this reference.

BLASTN output was processed using the filtering scripts of the 'cpDNA' pipeline (see Zenodo at https://doi.org/10.5281/zenodo.18911114). To maximise locus and sample retention, all filtering thresholds were set to zero, and the best match for each locus was selected based on bitscore. For loci comprising multiple exons, sequences were reconstructed by merging exons according to BLASTN coordinates of the best-match reference sequence. All recovered plastid loci were concatenated per sample and subsequently separated into per-locus FASTA files across samples.

All loci recovered after filtering were aligned independently using MAFFT v7.508 ("adjustdirection" and "auto" options) and trimmed with trimAL v1.4.1 using the "gappyout" method. A plastid phylogenetic tree was then inferred from the concatenated alignment of all genes using maximum likelihood in IQ-TREE v2.2.0.3, applying independent GTR + G models for each locus and assessing branch support with 1000 ultrafast bootstrap replicates.

2.3.2. Clade association and phasing

Hybrids have haplotypes inherited from different parental species and therefore show elevated numbers of SNPs (Nauheimer et al., 2021). Using the SNPs identified in section 2.2.2., we inferred allele divergence (AD; percentage of SNP sites across loci) and locus heterozygosity (LH; percentage of loci with SNPs) for the nuclear loci of each sample. High LH (>80%) and AD (>1%) are commonly used indicators of past hybridisation (Andermann et al., 2018; Kates et al., 2018; Nauheimer et al., 2021).

By mapping reads to references representing different parts of the phylogenetic tree, it is possible to assess whether samples have reads mapping in high proportions to multiple clade references together with high LH and AD, as is expected of hybrids (Fitzpatrick, 2012; Nauheimer et al., 2021). We selected nine samples as references in the first attempt (Supplementary Table S4). Reference samples were chosen to represent all major clades, especially those suspected to contain hybrids, while exhibiting low LH and AD values, making them unlikely to be hybrids themselves.

Samples were selected for phasing based on a combination of phylogenetic, morphological, and genomic indicators of potential hybrid origin. We first examined the ASTRAL tree, focusing on the *T. pinnatum* complex, and flagged samples that occupied unexpected phylogenetic positions or showed morphology differing from the majority in a clade or suggesting mixed ancestry. For these samples, we also assessed LH and AD values as additional support. We further included samples clustering closely with putative hybrids, but without high LH and AD values to avoid missing hybrid samples with weaker genomic signals. For samples outside the *T. pinnatum* complex, phasing selection relied primarily on LH and AD metrics.

Phasing as implemented in HybPhaser (Nauheimer et al., 2021) was used to map reads to the most likely parental clades to separate divergent haplotypes. As HybPhaser allows only two references per sample, reference selection in cases with multiple similarly supported candidates was based on a combination of consistency across preliminary analyses with varying filtering thresholds, normalised clade association values (accounting for read depth; see Supplementary Table S5), and morphological similarity. The same reference pair was applied across morphologically similar samples for consistency.

HybPiper and HybPhaser were subsequently run with the same settings as in section 2.2.2., except HybPhaser filtering thresholds were set to zero. The phased and unphased data were then merged, with unphased samples replaced by their corresponding phased samples. The resulting sequence lists were aligned and trimmed as described in section 2.2.2., and phylogenetic analyses were performed to generate an ASTRAL tree following the same pipeline as for the non-phased data.

The first phasing attempt was not entirely successful (Supplementary Fig. S2), so we repeated the analysis using a revised set of seven reference samples that more closely matched the haplotypes of the samples selected for phasing than the original reference set did (Supplementary Table S4; S6). The results presented below are based on the revised reference set.

To estimate branch lengths for the ASTRAL topology in substitution rates per site, we concatenated all loci with AMAS and analysed the resulting supermatrix in IQ-TREE under the GTR + F + G4 model, providing the ASTRAL tree as a fixed topology via −te and allowing IQ-TREE to optimise branch lengths and model parameters.

3. Results

3.1. Dataset assembly

3.1.1. Nuclear sequence assembly and data filtering

Using the adapted GoFlag-451 reference file, HybPiper recovered sequences for 396 of the 436 targeted loci across all 303 sequenced samples, although recovery per sample was highly variable (Supplementary Table S3). On average, individual samples contained sequences for 159 loci (range: 2–324), corresponding to an average recovered sequence length of 47,543 bp (range: 147 bp–138,870 bp). Across all samples, HybPiper reported 236 paralog warnings, affecting between 1 and 27 loci per sample (mean 6.1).

To improve data quality, 103 samples were excluded using HybPhaser based on the selected missing-data thresholds (Supplementary Fig. S3). After filtering, the retained dataset comprised 200 samples, with a mean recovered target sequence length of 86,696 (range: 37,604–171,241 bp), corresponding to 51% of the maximum target length.

Finally, 25 loci were excluded because they were flagged as

paralogous across samples (average SNP proportion >3.4%), and in addition, an average of 5.8 loci per sample (range 0–33; Supplementary Table S6).

3.1.2. Plastid assembly and data filtering

Using off–target reads from the 200 samples included in the nuclear dataset, we recovered 768 plastid sequences from 194 samples (97%) representing 17 loci (median summed locus length = 4,424 bp) by querying against the plastid reference file of 124 loci (Supplementary Table S7). After alignment and trimming, eight loci were excluded because their alignments contained fewer than three sequences. The plastid phylogenetic dataset was therefore inferred from the remaining nine loci (rnl, rns, rps7, rrn4.5, rrn5, trnA_UGC, trnI_GAU, trnR_ACG, trnV_GAC; 7.3%), with a combined alignment length of 6,533 bp, of which 316 sites were parsimony-informative (4.8%; Supplementary Table S8).

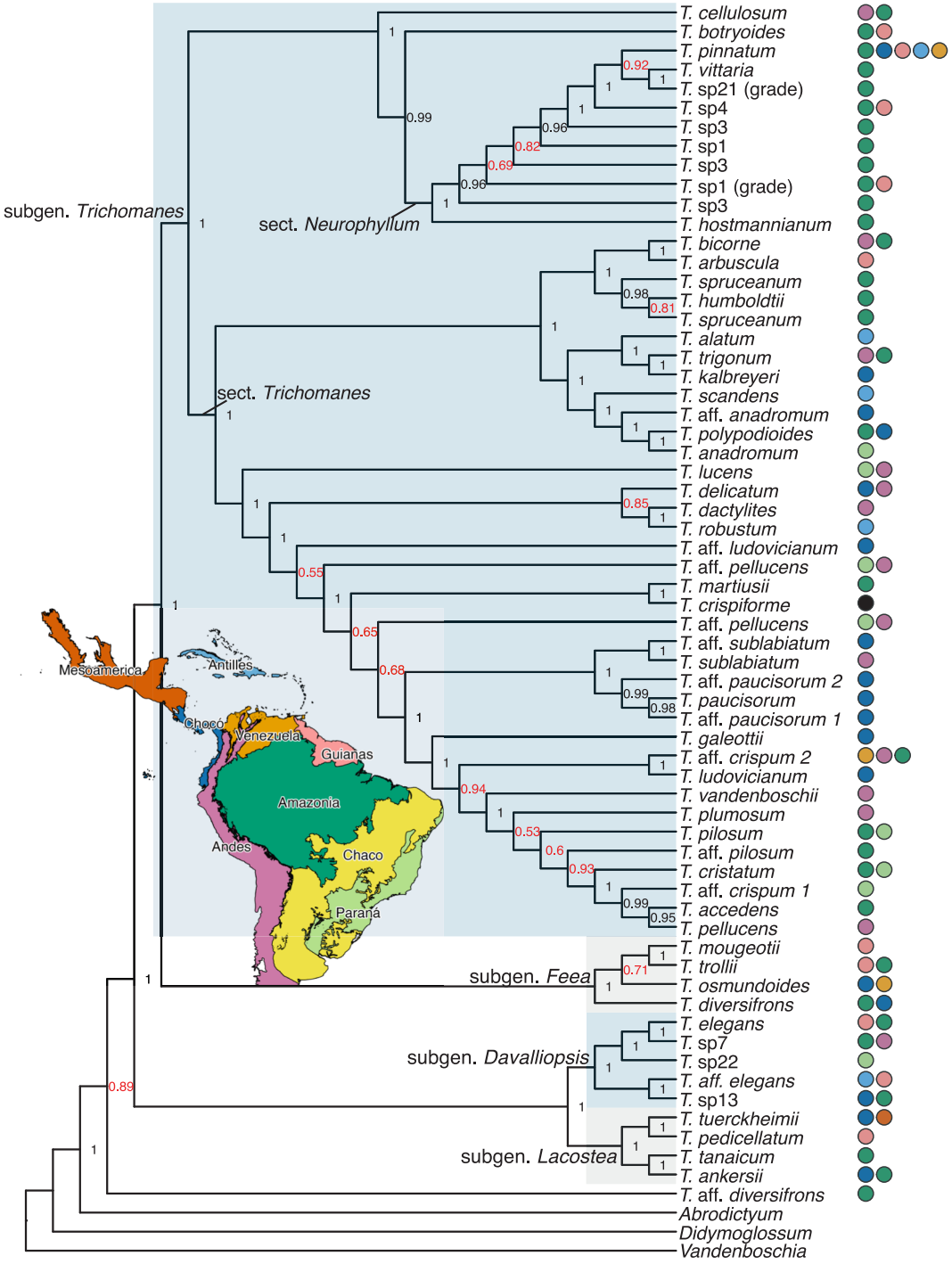

Fig. 2. Phylogenetic tree of Trichomanes (sensu PPG I) based on nuclear genomic data from 200 samples as inferred with ASTRAL-hybrid and collapsed to species. Node labels show the local posterior probability support values; values <0.95 are shown in red. Tip labels show species names followed by colours that indicate the regions (see inset; map from Frederiksen et al. (2025)) in which the corresponding samples were collected. For the complete tree with branch lengths in coalescent units and each sample shown separately, see Fig. S4. (For interpretation of the references to colour in this figure legend, the reader is referred to the web version of this article.)

3.2. Overall evolutionary relationships

All traditionally recognised subgenera (*Davalliopsis*, *Feea*, *Lacostea* and *Trichomanes*; Ebihara et al. 2006) were resolved as monophyletic with maximal support both in our nuclear tree (Fig. 2; Supplementary Fig. S3) and in our plastid tree (Supplementary Fig. S5). The two trees also agreed in that subgen. *Davalliopsis* and *Lacostea* were strongly supported as sister clades, and together they were sister to the strongly supported clade *Feea* + *Trichomanes*. Differences among the nuclear and plastid topologies emerged within subgenera. The description of the results below is mostly based on the nuclear tree because it was more robust (higher node support values; Fig. 2; Supplementary Figs. S4, S5).

Subgen. *Davalliopsis* was divided into five highly supported clades (Fig. 2, Supplementary Fig. S4). In subgen. *Lacostea*, all species were highly supported, with *T. pedicellatum* + *T. tuerckheimii* being sister to *T. ankersii* + *T. tanaicum*. Within subgen. *Feea*, all species were resolved as monophyletic with high support but their relationships within the clade remained uncertain: *T. osmundoides* was only moderately supported as sister to *T. mougeotii* + *T. trollii* in the nuclear tree, and in the plastid tree it was resolved as sister to *T. diversifrons*.

Most of the sequenced species were in subgen. *Trichomanes*, which in the nuclear tree was split into two strongly supported clades. One of these contained the entire *T. pinnatum* complex (*T. pinnatum, T. vittaria,* and all the numbered morphs), which was resolved as monophyletic and sister to a monophyletic *T. hostmannianum*. These together are here referred to as sect. *Neurophyllum* (Presl) Moore. *Trichomanes cellulosum*, followed by *T. botryoides,* were sister to the rest of the clade. In the plastid tree, *T. cellulosum* was recovered as the earliest–diverging lineage within subgen. *Trichomanes*, sister to all remaining taxa, whereas *T. botryoides* was resolved as sister to sect. *Trichomanes* (Supplementary Fig. S5). The lability of their phylogenetic position mirrors their unusual morphology: *T. botryoides* with its simple fertile leaf resembles subgen. *Feea*, while *T. cellulosum* has finely divided leaves reminiscent of *Abrodictyum*.

The second clade of subgen. *Trichomanes* (here referred to as sect. *Trichomanes*) was further split into two maximally supported subclades in both the nuclear and the plastid tree. One subclade consists of species that typically grow either terrestrially in Amazonian white sand forests (*T. arbuscula*, *T. bicorne*, *T. humboldtii*, and *T. spruceanum*) or as epiphytes (or on rocks) with divergent distributions across tropical America (*T. alatum*, *T. anadromum*, *T. kalbreyeri*, *T. polypodioides*, *T. scandens*, and*T. trigonum*).

In the second subclade, *Trichomanes lucens* (a distinctive epiphytic species) was strongly supported as sister to the rest of the subclade. The subclade further contains both terrestrial and epiphytic species, but these were arranged into a topology that did not correspond with substrate or morphology in any obvious way. Many nodes were only moderately supported, and this subclade is also where the topologies differed most between our nuclear and plastid trees. Importantly, this subclade contains all the species that show high morphological similarity to the type species of the genus (*T. crispum*). This includes the western African *T. crispiforme*, which was resolved as sister to the Amazonian *T. martiusii.* Unfortunately, our sampling does not include any *T. crispum* from the type area of the species (Lesser Antilles), and since the specimens from elsewhere got split up by geographical region (Amazonia vs. Brazilian Atlantic coast) into two different subclades, the position of true *T. crispum* remains uncertain (hence the use of aff. in the identifications of our sampled specimens).

3.3. Trichomanes pinnatum and other complexes

A central aim of our study was to clarify species delimitation within the morphologically variable and geographically widespread *T. pinnatum* complex. The phylogenetic analyses recovered a well-defined core clade consisting of *T. pinnatum* samples originating from a very large geographical area but showing little genetic differentiation (Fig. 2; Supplementary Fig. S4). The samples of *T.* sp11 were included in this clade but they were scattered among other specimens rather than forming a coherent group.

Trichomanes vittaria, which is characterised by a simple rather than pinnate fertile leaf, was in the nuclear tree resolved as a strongly supported monophyletic group, but successively sister to this clade was a grade of specimens that are morphologically intermediate between *T. vittaria* and *T. pinnatum* (referred to as *T.* sp21). *Trichomanes* sp4 was resolved as monophyletic with strong support. This contrasted with *T.* sp1 and *T.* sp3, which were mixed with each other and formed a grade successively sister to the (((*T. vittaria* + *T.* sp21) *T. pinnatum*) *T.* sp4) clade. The topology of the plastid tree is quite different: the core consists not only of *T. pinnatum* and *T.* sp11, but mixed within it are also *T.* sp1, *T.* sp3 and *T.* sp4, with *T. vittaria* and *T.* sp21 forming a mixed grade successively sister to the core clade (Fig. S5).

In the nuclear tree, most species within sect. *Trichomanes* were resolved as monophyletic with strong support, but a few appeared paraphyletic or polyphyletic (Fig. 2; Supplementary Fig. S4): *T. anadromum, T. bicorne, T. crispum, T. ludovicianum, T. pellucens, T. pilosum*, and *T. spruceanum*. The clade consisting of *T. paucisorum* and *T.* aff. *paucisorum* is morphologically heterogeneous and could contain more than one species.

3.4. Hybridisation

To assess if hybridisation could explain some of the observed phylogenetic relationships, we first examined locus heterozygosity (LH) and allele divergence (AD) of the *Trichomanes* samples (Fig. 3). In most cases, hybrid signal was low (LH $<$ 50% and AD $<$ 1%). Only five samples reached a moderate degree of hybrid signal (LH $>$ 80% and AD $>$ 1%), and all of these were chosen for phasing to test for different origins of the maternal and paternal genetic material. In addition, we phased another 30 samples that mostly represented the *T. pinnatum* complex. In the phased accessions, LH ranged 49–89% and AD ranged 0.7–1.4% (Fig. 3; Supplementary Table S4).

Species of sect. *Neurophyllum* had, on average, significantly higher LH values than species of sect. *Trichomanes* and the subgenera *Lacostea* and *Davalliopsis*. In *Feea*, the unusually high LH values of *T. trollii* caused a long upward tail in the LH value distribution, with the result that the average did not differ from that in *Neurophyllum* (Fig. 4; see also Fig. 3). Although AD values also varied, they did not differ significantly among subgenera/sections. Overall, species of sect. *Neurophyllum* had significantly higher LH than species of *Trichomanes* not in *Neurophyllum*, but AD did not differ significantly (Supplementary Fig. S6).

In most of the samples selected for phasing, the reads mapped unambiguously and in high proportions to two reference clades, indicating that the samples were hybrids between lineages in the respective clades (Fig. 4, Supplementary Table S9). The proportion of reads mapping to each reference ranged between 1:1 (which is consistent with diploidy or symmetric polyploidy) to 7:1 (which is expected from highly unequal copy numbers or hybridisation and repeated backcrossing; Table 1).

To assess possible hybridisation among the evolutionary lineages, we produced a phylogenetic tree where each of the phased samples occupied two terminals, one corresponding to each of the two recovered haplotypes (Fig. 5; Supplementary Fig. S7). This revealed that four of the five morphs in the *T. pinnatum* complex are likely hybrids: *T.* sp1, *T.* sp3, *T.* sp4, and *T.* sp21.

The phased specimens of *T.* sp1 split in the phylogenetic analysis such that one haplotype formed a clade as sister to *T. hostmannianum,* while the other haplotype formed a grade successively sister to the clade that contains all the other morphs of the *T. pinnatum* complex, including *T. pinnatum* and *T. vittaria* (except one specimen was resolved as sister to only *T. pinnatum*). The phased specimens of *T.* sp3 behaved in a less cohesive manner: one haplotype formed a grade successively sister to *T. hostmannianum,* whereas the other was scattered, with each sample

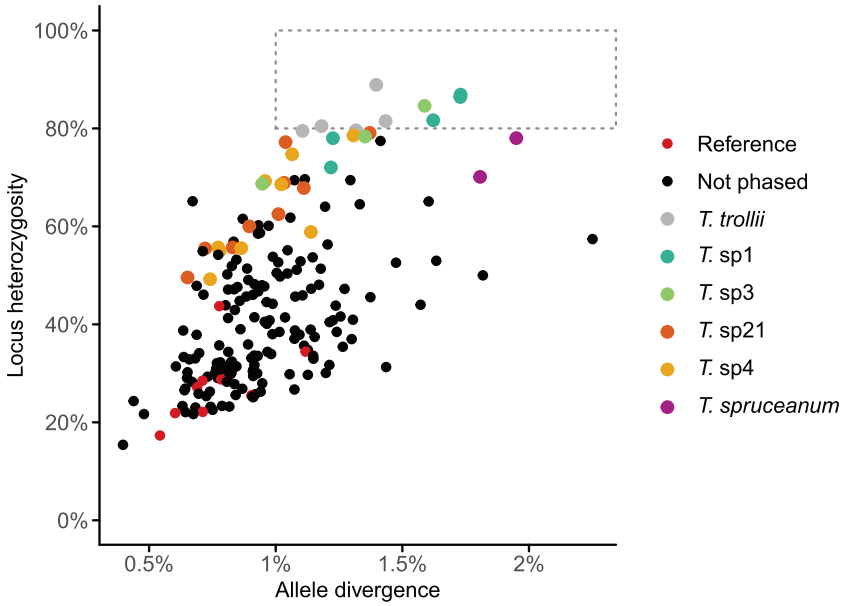

Fig. 3. Locus heterozygosity and allele divergence for all samples of *Trichomanes*. Colours identify samples that were used as references in phasing as well as putative hybrids (the latter are shown with larger dots).

resolved to a different part of the *T. pinnatum* complex (except for one haplotype of one sample, which was lost during HybPhaser filtering; see Supplementary Fig. S2 for placement in phylogenetic tree during the first phasing attempt).

The samples representing *T.* sp21 are morphologically intermediate between *T. pinnatum* and *T. vittaria*, and indeed one of the haplotypes remained as a grade successively sister to *T. vittaria*, while the other formed a clade sister to *T. pinnatum* (Fig. 5; Supplementary Fig. S7). Interestingly, *T.* sp4 was also associated with both *T. pinnatum* and *T. vittaria*, but in this case each haplotype was resolved as an earlier diverging lineage, sister to a clade that includes not only all samples of *T. pinnatum* or *T. vittaria*, respectively, but also the haplotypes of *T.* sp21 that were phased to these species (Fig. 5; Supplementary Fig. S7). The haplotypes of *T.* sp4 phased against the *T. pinnatum* reference were monophyletic, and those phased against the *T. vittaria* reference almost so. The exception (Lehtonen 983) had low read depth prior to phasing (37,000 reads), which may explain why they were resolved as earlier diverging relative to the others and was sister *T. pinnatum* and the haplotypes that were phased to *T. pinnatum*.

In sect. *Trichomanes*, we phased *T. spruceanum,* which showed both high locus heterozygosity (LH) and high allele divergence (AD). Its haplotypes split into two clades with strong support, one sister to *T. bicorne* Hook., and the other to *T. humboldtii* (Bosch) Lellinger (Fig. 5; Supplementary Fig. S7).

Trichomanes trollii of subgen. *Feea* obtained some of the highest LH values in our dataset, but in the phased tree the two haplotypes stayed together as a clade (Fig. 5; Supplementary Fig. S7). Interestingly, while all analyses confirmed the sister relationship between *T. trollii* and *T. mougeotii*, the positions of *T. diversifrons* and *T. osmundoides* differed among the three trees (original nuclear, phased nuclear and plastid; Supplementary Figs. S2, S5, S7).

4. Discussion

4.1. New view on subgeneric relations

With both nuclear and plastid data, we recovered relationships between subgenera that had already been proposed by Ebihara et al. (2006, 2007) but obtained very low support at the time (bootstrap < 50%). Specifically, our results strongly support subgen. *Trichomanes* as sister to *Feea*, contrasting with studies that placed subgen. *Trichomanes* as sister to a clade containing all remaining subgenera (*Davalliopsis*, *Feea* and *Lacostea*; Dubuisson et al., 2022, 2003). We consider the relationships as resolved in our analyses robust, as they are based on a dense taxon sampling, in-depth target capture nuclear data (326 loci), and some plastid data (nine loci). The close association between the subgenera *Feea* and *Trichomanes* also makes sense in that they share a similar overall pinnatifid to once pinnate leaf structure, which contrasts with the highly divided leaves of *Davalliopsis* and the climbing leaves of *Lacostea*. *Feea* and *Trichomanes* sect. *Neurophyllum* also share a tendency towards leaf dimorphism.

We took into use section *Neurophyllum* (Presl) Moore for the *T. pinnatum* complex + *T. hostmannianum*, and section *Trichomanes* for the other main clade in the subgenus to acknowledge the deep split within subgen. *Trichomanes*. It would also be possible to recognise the distinction at the subgenus level, but here we chose to use the existing section rank and the already established subgenus delimitation (Dubuisson et al., 2022).

Especially *T. cellulosum*, but also *T. botryoides*, complicate the matter when subgen. *Trichomanes* is further divided. Morphologically, *T. cellulosum* has little in common with the species that form the core of sect. *Neurophyllum,* and in our plastid tree *T. cellulosum* was not resolved with core *Neurophyllum* but instead appeared as sister to the entire subgen. *Trichomanes.* This contrasts with both our nuclear tree and the plastid-based tree of Dubuisson et al. (2022). Since our plastid data were obtained as a by-product of the nuclear target capture, it is possible that the difference emerged due to low data quality. However, aside from this conflict, the backbones of the plastid and nuclear trees show strong overall congruence. Taken together, the inconsistent placement of. *T. cellulosum*, along with the uncertain position of *T. botryoides*, indicate that their relationships remain unresolved and merit further study.

The only African specimen in our study (*T. crispiforme* from Gabon) resolved to sect. *Trichomanes*, in agreement with its position (under the synonym name *T. crenatum*) in the tree of Dubuisson et al. (2022). However, while our analyses resolved it as sister to *T. martiusii*, in the previous tree it was sister to a clade containing *T. accedens, T. dactylites, T. pilosum* and *T. vandenboschii*, which in our tree were split into two other subclades.

Although our analyses suggest a different phylogenetic position for subgen. *Trichomanes* than that recovered by Dubuisson et al. (2022),

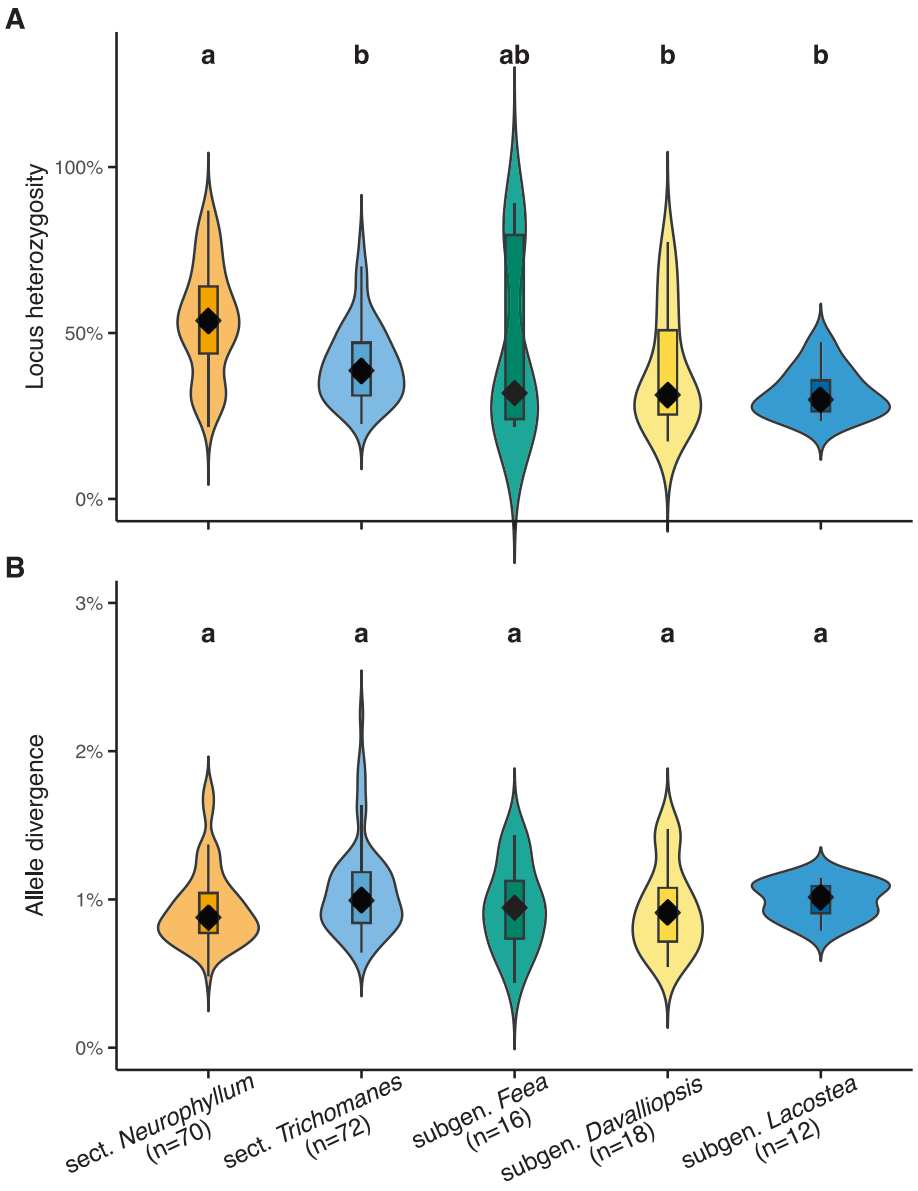

Fig. 4. Signal of putative hybridisation from locus heterozygosity (A) and allele divergence (B) across the subgenera and sections of *Trichomanes*. The width of the violin represents the frequency of data points. Diamonds indicate the median, the box indicates the interquartile range (IQR), and whiskers represent the 95% confidence interval. Differences in the mean values were assessed by Kruskal-Wallis test; $P = 6.2{\cdot}10^{-7}$ for panel A and $P = 0.095$ for panel B. Letters (a vs. b) indicate significant differences ($P < 0.05$) between groups based on Wilcoxon test after Holm-Bonferroni adjusted tests of significant pair-wise differences. n = number of samples.

Table 1
Reads matching unambiguously to each reference from the clade association analysis (see also Supplementary Table S9). For each species, the table summarises the observed mapping ratios across samples. Avg. ratio raw (range) reports the mean uncorrected read ratio (ref. 1: ref. 2) with its sample range. Avg. ratio inferred (range) reports the interpreted allelic ratio derived from raw data, along with the range of plausible inferred values. These ratios provide indirect evidence for ploidy level and genome composition but do not uniquely distinguish among alternative configurations with similar expected ratios (e.g. diploid vs. balanced tetraploid).

Taxon	No. samples	Reference 1	Reference 2	Avg. ratio raw (range)	Avg. ratio inferred (range)
T. sp1	5	*T. pinnatum*	*T. hostmannianum*	2.13:1 (1.75–2.46:1)	2:1 (2:1–5:2)
T. sp3	3	*T. pinnatum*	*T. hostmannianum*	1.82:1 (1.70–1.96:1)	2:1 (3:2–2:1)
T. sp4	10	*T. pinnatum*	*T. vittaria*	2.36:1 (1.62–2.90:1)	2:1 (3:2–3:1)
T. sp21	9	*T. pinnatum*	*T. vittaria*	1.37:1 (1.12–1.61:1)	1:1 (1:1–3:2)
T. trollii	5	*T. mougeotii*	*T. osmundoides*	6.07:1 (4.97–6.61:1)	6:1 (5:1–7:1)
T. spruceanum	2	*T. bicorne*	*T. humboldtii*	2.18:1 (1.26–3.09:1)	2:1 (1:1–3:1)

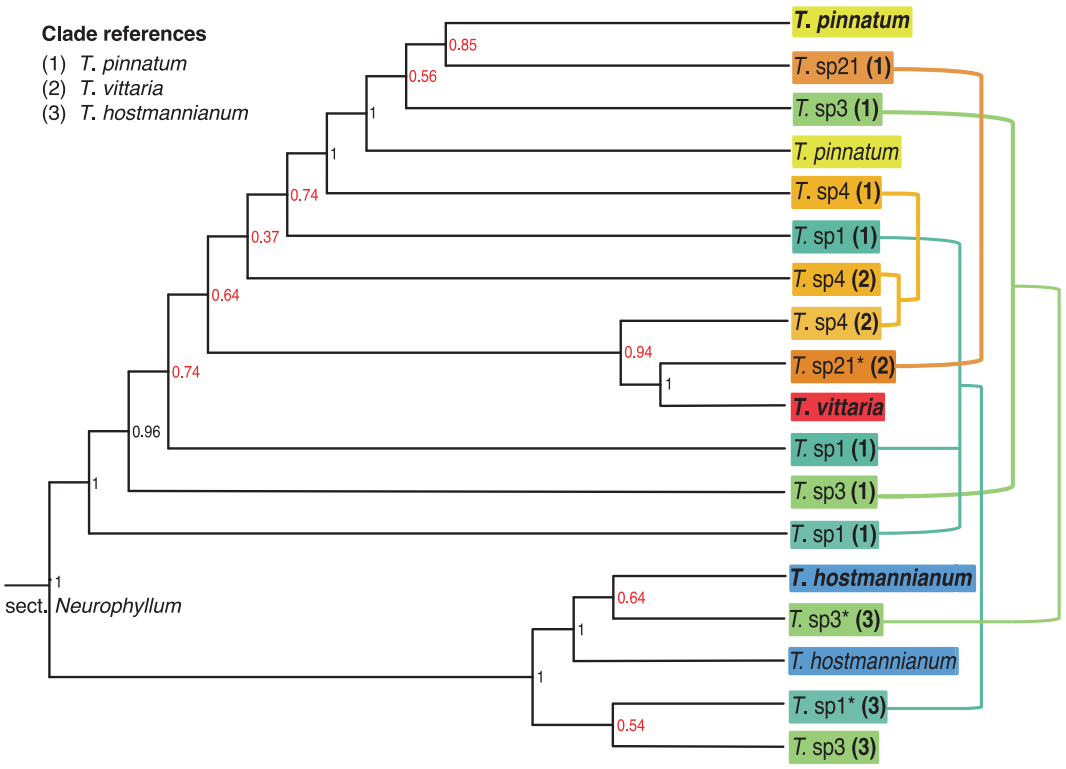

Fig. 5. Phylogenetic tree of *Trichomanes* sect. *Neurophyllum* as inferred with ASTRAL-hybrid based on phased nuclear data. Accessions with hybrid signal were phased and each of the resulting two haplotypes was included as a separate terminal in the analysis. The final tree was simplified by collapsing groups of the same species or numbered morph (those marked by * are collapsed grades rather than clades). Node labels show the local posterior probability support values; values < 0.95 are in red. Lines on the right-hand side visualise hybrid parentage by connecting the two haplotypes of the hybrid morphs, and their colour mixing approximates genomic mixing. The brackets with a number refer to the species the sample was phased against as indicated in the upper left corner. For full details on phasing proportions, see Supplementary Table S9. For the phased tree of the entire genus *Trichomanes* with branch lengths and each sample shown separately, see Supplementary Fig. S7. (For interpretation of the references to colour in this figure legend, the reader is referred to the web version of this article.)

their conclusions about character evolution remain valid. They interpreted catadromous venation and epitactic sori as apomorphies of subgen. *Trichomanes,* and this conclusion is also consistent with our topology. Indeed, placing subgen. *Feea* as sister to subgen. *Trichomanes* brings morphologically similar groups together, as *Neurophyllum* and *Feea* are the two clades within the genus that most often exhibit dimorphic leaves and pantotactic sori.

4.2. *Trichomanes pinnatum* complex explained by hybridisation

Traditionally, *T. pinnatum* has been considered a widespread and morphologically variable species that includes our morphs sp1, sp4, sp11 and sp21, while specimens of our morph sp3 have been identified as *T. hostmannianum*. Our genomic analyses suggest that this is an oversimplification, as the phylogenetic analyses recovered a rather intricate internal structure for this complex. The numbered morphs represent four different kinds of evolutionary background: clearly self-maintaining species with a hybrid origin in the distant past (*T.* sp1 and *T.* sp4), more recent hybridisation possibly leading to speciation (*T.* sp21), occasional spontaneous hybridisation (*T.* sp3) and within-species morphological variation without genetic signal (*T.* sp11).

Field inventories in Amazonia have long treated *T.* sp1 and *T.* sp4 as distinct species, because they are morphologically distinct, widespread, abundant, and associated with consistent environmental conditions (Cárdenas et al., 2007; Lehtonen et al., 2021; Tuomisto et al., 2002; HT, pers. obs). In contrast, individuals of *T.* sp21 are rarer and geographically more restricted, and they have been considered hard-to-identify intermediates between *T. pinnatum* and *T. vittaria* (HT, pers. obs.). Our genomic analyses not only confirmed that all three are genetically distinct from *T. pinnatum* s.str. but also suggested that they have a hybrid origin that connects them with *T. pinnatum*. Haplotype phasing and the position of the haplotypes in the phased phylogenetic tree suggested that the oldest hybridisation event in this group was between *T. hostmannianum* and an early (now probably extinct) common ancestor of the *T. pinnatum* + *T. vittaria* + *T.* sp21 clade, which gave rise to *T.* sp1. A later hybridisation event between *T. pinnatum* and a common ancestor of the *T. vittaria* + *T.* sp21 clade gave rise to *T.* sp4, and one or more even more recent hybridisation events between *T. pinnatum* and the already differentiated *T. vittaria* gave rise to *T.* sp21.

Out of these three hybrids, *T.* sp4 is the clearest candidate for a species that originated from a single hybridisation event: both of its phased haplotypes were resolved as monophyletic, except for one sample with short sequence length and correspondingly uncertain phylogenetic position (Nauheimer et al., 2021). Only one of the haplotypes was monophyletic for *T.* sp1 (the one phased to *T. hostmannianum*) and *T.* sp21 (the one phased to *T. pinnatum*), the other one was paraphyletic in each case. This could be due to short sequence length, incomplete lineage sorting after multiple introgression events or asymmetric introgression (Ross, 2014; Yasuda et al., 2015).

The case of *T.* sp3 is quite different: it forms no clades in either the original or the phased tree. The haplotype phased to *T. hostmannianum* is partly sister to the *T. hostmannianum* clade and partly mixed with *T. hostmannianum* itself, and the haplotype phased to *T. pinnatum* got spread across the entire *T. pinnatum* complex. This gives the impression of spontaneous hybrids being formed repeatedly in different places where both parent species co-occur. In ecological inventories, the identification of this morph has been inconsistent: sometimes specimens have been considered to represent *T. hostmannianum,* sometimes they have been thought of as distinct.

After having segregated the hybrids, we are left with a core *T.*

pinnatum that is morphologically less variable than before but geographically equally widespread. It still contains forms with different leaf shapes (including *T.* sp11 with unusually long and narrow sterile leaves), but these were mixed within the clade without any obvious relationship between morphology and genetic relatedness, suggesting that *T.* sp11 is not genetically distinct from typical *T. pinnatum*.

It is interesting that core *T. pinnatum* is a putative parent of all hybrids we identified in this complex, although in the case of *T.* sp1, the hybridisation appears to have pre-dated the separation between *T. pinnatum* and *T. vittaria*. This suggests sufficient ecological and spatial overlap with congeners to allow interbreeding, and weak barriers to interspecific cross-fertilisation (Sigel, 2016).

The branch lengths in the phylogenetic trees suggest that there is little genomic variation in the form of substitutions per site within *T. pinnatum* s.s. despite a huge distributional area, and the existing variation does not seem to be geographically structured. Consequently, we propose that *T. pinnatum* approaches panmixia (random mating across its entire distribution with little restriction to gene flow among populations; (Walton et al., 2025; Weismann, 1883). This requires high dispersal ability, large population size, and extensive connectivity. Although it is known that minute fern spores have high long-distance dispersal ability (Brock, 2025; Perrie and Brownsey, 2007; Tryon, 1970; Wolf et al., 2001), it is not clear why *T. pinnatum*, more than other *Trichomanes* species, shows this pattern and is able to span most of the American tropics with remarkably little genetic variation.

4.3. Detecting hybrid origins

Interestingly, we found that low allele divergence (AD) and locus heterozygosity (LH) does not necessarily mean that a specimen is not a hybrid. Our phasing analyses clearly suggested that *Trichomanes* sp1, *T.* sp3, *T.* sp4 and *T.* sp21 are hybrids, but none of them showed particularly high values of LH or AD when compared to the values that are generally referred to as indicating hybridisation, namely LH $>$ 80 and AD $>$ 1 (Bloesch et al., 2022; Nauheimer et al., 2021). The highest LH values were observed in *T.* sp1 and *T.* sp3 (69–87%), with the values in *T.* sp4 and *T.* sp21 generally lower (49–79%, with one sample as low as 33%). Of the *Neurophyllum* samples that phasing suggested to be of hybrid origin, 60% had AD $<$ 1%, some as low as 0.7%.

Out of the two measures, LH did provide a clearer signal of hybridisation in our dataset. This was also reflected in that the LH values observed in *Neurophyllum* were higher than in the other subgenera/sections, except for *Feea*. *Neurophyllum* species also had many accessions that mapped to multiple clade references, which indicates hybridisation or introgression (Nauheimer et al., 2021).

Contrary to expectation, the species with the highest average LH in our dataset (*T. trollii*) appears not to be a hybrid: it showed little affinity to the other species in the analysis, and both of its haplotypes were resolved into the same well–supported clade in the phased nuclear tree. Since all known species of subgen. *Feea* were included in our analyses, we must assume that if the high LH in *T. trollii* does indicate past hybridisation, it involved either species that are not known to science and may now be extinct (ghost introgression; Ottenburghs, 2020) or polyploidy not involving hybridisation, as proposed for similar cases before (Nauheimer et al., 2021). The species with the strongest combined hybrid signal (both high LH and high AD) within sect. *Trichomanes* (*T. spruceanum*) was indeed found to be a hybrid. Its putative parent species are *T. bicorne* and *T. humboldtii* from the same subclade, which is somewhat surprising as one might expect hybridisation between close relatives to result in lower AD than hybridisation between more remotely related parents (Keskiniva et al., 2024).

Phasing ratios, together with conflicting reports of diploidy (Walker, 1985) and tetraploidy (Bierhorst, 1975) in *T. pinnatum*, indicate that multiple hybridisation scenarios are plausible (Table 1). Across hybrids *T.* sp1, *T.* sp3, and *T.* sp4, phasing patterns reveal an ~2:1 or ~3:1 ratio of reads assigned to *T. pinnatum* versus the second parent (Table 1). Under diploidy, such ratios suggest introgression via backcrossing to *T. pinnatum*, whereas under tetraploidy they align with expectations for F1 hybrids. In contrast, *T.* sp21 has an ~1:1 ratio, which indicates an F1 hybrid under diploidy but suggests introgression via backcrossing to *T. vittaria* under a tetraploid scenario. The predominance of ~2:1 rather than ~3:1 ratios, expected for clean diploid introgression could therefore indicate tetraploidy in *T. pinnatum*. Alternatively, these ratios may reflect intermediate ploidy levels, such as triploidy or hexaploidy, as proposed for similar patterns observed in the *Christella dentata* (Forssk.) Brownsey & Jermy complex (Bloesch et al., 2022). Morphological patterns provide additional, although indirect, support for hybrid origins. It can be hypothesised that *T.* sp1, *T.* sp4 and *T.* sp21 show hybrid vigour (Chen, 2010; Fridman, 2015). Especially *T.* sp1 is much larger and more robust than any other species of sect. *Neurophyllum*, while *T.* sp4 and *T.* sp21, though not as large, still tend to be taller than their putative parents. On the other hand, specimens of *T.* sp3 tend to be rather small when compared to their putative parents.

Ultimately, resolving these evolutionary histories will require targeted cytological work, as phasing ratios alone are insufficient. Perfect phasing is achievable only when reference sequences match the true parents and when mutation or recombination have not concealed allele identities. In practice, mismatches arise due to divergence, heterozygosity, or differences in sequence length and locus coverage (Nauheimer et al., 2021). For example, *T.* sp1 likely involves an unsampled parent, as it phases to a clade including both *T. pinnatum* and *T. vittaria*. Moreover, deviations (e.g., 2:1 instead of 1:1 or 3:1) may reflect incomplete lineage sorting, backcrossing, gene duplication or loss, or ploidy differences among progenitors (Bloesch et al., 2022; Nauheimer et al., 2021; Tseng et al., 2024).

4.4. Cryptic species

We were able to confirm most species circumscriptions within each subgenus (Dubuisson et al., 2022, 2003; Ebihara et al., 2006; Lellinger, 1994; Lellinger and Windisch, 1994), while also addressing some unresolved questions from previous studies. Several species within subgen. *Trichomanes* sect. *Trichomanes* turned out to be paraphyletic or even polyphyletic, suggesting that their circumscriptions need to be revised. The corresponding specimens did not stand out as having high hybrid signal, however, so they are maybe more likely to represent cryptic species than hybrids.

One notable case was *T. ankersii* within subgenus *Lacostea*, which has previously been resolved as paraphyletic and several species with affinity to *T. ankersii* have been suggested (Dubuisson et al., 2022). Our analyses recovered *T. ankersii* as monophyletic but split into two well-supported clades (one Amazonian and one Andean/Mesoamerican), separated by substantial genetic divergence. This pattern raises the possibility of cryptic speciation (Paris et al., 1989; Yi et al., 2023). Consistent with Dubuisson et al. (2022), we also found *T. ankersii* as sister to *T. tanaicum* and *T. pedicellatum* as sister to *T. tuerckheimii*, a result that is intriguing given morphological similarities between species pairs that do not immediately align with these phylogenetic relationships.

The placement of *T. osmundoides* within subgen. *Feea* remains ambiguous. In Ebihara et al. (2007) it grouped with *T. mougeotii*, but in Dubuisson et al. (2022) it grouped with *T. diversifrons*. In our analyses we find a different topology in each of the three phylogenetic analyses (original nuclear, phased nuclear, plastid), but all received low support. Like *T. ankersii, T. diversifrons* was also split into two subclades, one in Amazonia and the other one in Mesoamerica and the Pacific coast of Ecuador.

Finally, our results for *T. elegans* (Subgen. *Davalliopsis*) align with those of Dubuisson et al. (2022), confirming two well-supported clades that correspond to northern and southern distributions. The northern clade includes Amazonian populations, whereas the southern clade extends into the Andean region. Our analyses divided *T. elegans* even more

finely into five highly supported clades that differ in geographical distribution. Since only two species names (*T. elegans* and *T. resinosum*) have been widely applied to this group, some of the clades may represent undescribed species.

5. Conclusions

Our study provides the first nuclear phylogenomic framework for *Trichomanes* and resolves key relationships within the genus, recovering subgenus *Trichomanes* as sister to subgen. *Feea*. Guided by morphology and phylogenetic placement, we further propose reinstating section *Neurophyllum* within subgen. *Trichomanes* comprising *T. pinnatum*, *T. vittaria* and *T. hostmannianum*. This section, which includes the taxonomically challenging *T. pinnatum* complex, has significantly elevated heterozygosity compared to the other section and subgenera. Through haplotype phasing, we show that hybridisation has played an important role in shaping diversity within this group, producing several distinct outcomes: ancient hybrid-origin lineages that are now self-maintaining (*T.* sp1 and *T.* sp4), recent or ongoing hybridisation (*T.* sp21), recurrent spontaneous hybrids (*T.* sp3), and a geographically widespread parental species approaching panmixia (*T. pinnatum* s.s.). Evidence for possible ploidy heterogeneity highlights the need for targeted cytological work to clarify how these lineages originated and are maintained.

Across the genus, species boundaries are generally supported yet refined, and we uncover previously unrecognised diversity and clarify the placement of taxa not included in previous studies. The implications of the present results for nomenclature will be the topic of a separate taxonomic treatment. Overall, our study shows that both divergence and reticulation have shaped the evolutionary history of *Trichomanes* more profoundly than previously recognised, establishing a strong foundation for future systematic and evolutionary work.

CRediT authorship contribution statement

Laura Kragh Frederiksen: Writing – original draft, Visualization, Software, Formal analysis, Data curation, Conceptualization. **Jami Sundström:** Writing – review & editing, Conceptualization. **Wolf L. Eiserhardt:** Writing – review & editing, Supervision, Formal analysis. **Hanna Tuomisto:** Writing – review & editing, Visualization, Supervision, Funding acquisition, Data curation, Conceptualization.

Declaration of generative AI and AI-assisted technologies in the writing process

During the preparation of this work, Microsoft Copilot was used to write R code for generating the figures and python and unix code to reformat the headers of the plastid data and reference genome. After using this tool, the authors reviewed and edited the content as needed and take full responsibility for the content of the published article.

Funding

Funding from Aarhus University Research Foundation (grant AUFFE-2023-7-3 to HT), Danish National Research Foundation (grant DNRF179 to HT), and Research Council of Finland (grant 351460 to HT) is gratefully acknowledged.

Declaration of competing interest

The authors declare that they have no known competing financial interests or personal relationships that could have appeared to influence the work reported in this paper.

Acknowledgements

We are grateful to all the people who collected plants in the tropics and thereby made this study possible, especially Mirkka Jones, Samuli Lehtonen, Gabriel Moulatlet, and the late Benjamin Øllgaard and Paulo Windisch. We thank the TUR herbarium and Michael Kessler from Z for providing silica-dried plant samples, and AAU, BR, TUR and U for permission to take DNA samples from their herbarium specimens. All the computing for this project was performed on the GenomeDK cluster, and we thank GenomeDK and Aarhus University for providing computational resources and other support. We thank Malin Camilla Håkansson for DNA extraction and library preparation, and William J. Baker for providing crucial information on the pipeline for recovering plastid sequences.

Appendix A. Supplementary material

Supplementary material to this article can be found online at https://doi.org/10.1016/j.ympev.2026.108674.

Data availability

Sequence data has been deposited in the NCBI Sequence Read Archive under the BioProject PRJNA1404974 with SRA accessions SRR36992491 – SRR36992690. Scripts used to conduct the analysis, including output trimmed alignment and tree files are deposited in the Zenodo data repository at https://doi.org/10.5281/zenodo.18911114.

References

Abbott, R., Albach, D., Ansell, S., Arntzen, J.W., Baird, S.J.E., Bierne, N., Boughman, J., Brelsford, A., Buerkle, C.A., Buggs, R., Butlin, R.K., Dieckmann, U., Eroukhmanoff, F., Grill, A., Cahan, S.H., Hermansen, J.S., Hewitt, G., Hudson, A.G., Jiggins, C., Jones, J., Keller, B., Marczewski, T., Mallet, J., Martinez-Rodriguez, P., Möst, M., Mullen, S., Nichols, R., Nolte, A.W., Parisod, C., Pfennig, K., Rice, A.M., Ritchie, M.G., Seifert, B., Smadja, C.M., Stelkens, R., Szymura, J.M., Väinölä, R., Wolf, J.B.W., Zinner, D., 2013. Hybridization and speciation. J. Evol. Biol. 26, 229–246. https://doi.org/10.1111/j.1420-9101.2012.02599.x.

Abreu, F.P.de, Gonzatti, F., Bahima, I.A., de Souza-Chies, T.T., Kaltchuk-Santos, E., 2024. A global review of chromosome number and genome size for the filmy ferns family (Hymenophyllaceae, Polypodiopsida). Rodriguésia 75, e00552023. https://doi.org/10.1590/2175-7860202475038.

Andermann, T., Fernandes, A.M., Olsson, U., Töpel, M., Pfeil, B., Oxelman, B., Aleixo, A., Faircloth, B.C., Antonelli, A., 2018. Allele phasing greatly improves the phylogenetic utility of ultraconserved elements. Syst. Biol. https://doi.org/10.1093/sysbio/syy039.

Andrews, S., 2010. FastQC: A Quality Control Tool for High Throughput Sequence Data.

Balakrishnan, R., 2005. Species concepts, species boundaries and species identification: a view from the tropics. Syst. Biol. 54, 689–693. https://doi.org/10.1080/10635150590950308.

Bankevich, A., Nurk, S., Antipov, D., Gurevich, A.A., Dvorkin, M., Kulikov, A.S., Lesin, V. M., Nikolenko, S.I., Pham, S., Prjibelski, A.D., Pyshkin, A.V., Sirotkin, A.V., Vyahhi, N., Tesler, G., Alekseyev, M.A., Pevzner, P.A., 2012. SPAdes: a new genome assembly algorithm and its applications to single-cell sequencing. J. Comput. Biol. 19, 455–477. https://doi.org/10.1089/cmb.2012.0021.

Barrington, D.S., Haufler, C.H., Werth, C.R., 1989. Hybridization, reticulation, and species concepts in the ferns. Am. Fern J. 79, 55–64. https://doi.org/10.2307/1547160.

Bickford, D., Lohman, D.J., Sodhi, N.S., Ng, P.K.L., Meier, R., Winker, K., Ingram, K.K., Das, I., 2007. Cryptic species as a window on diversity and conservation. Trends Ecol. Evol. 22, 148–155. https://doi.org/10.1016/j.tree.2006.11.004.

Bierhorst, D.W., 1975. The apogamous life cycle of trichomanes pinnatum—a confirmation of Klekowski's predictions on homoeologous pairing. Am. J. Bot. 62, 448–456. https://doi.org/10.1002/j.1537-2197.1975.tb14069.x.

Bloesch, Z., Nauheimer, L., Almeida, T.E., Crayn, D., Field, A.R., 2022. HybPhaser identifies hybrid evolution in australian thelypteridaceae. Mol. Phylogenet. Evol. 173, 107526. https://doi.org/10.1016/j.ympev.2022.107526.

Bolger, A.M., Lohse, M., Usadel, B., 2014. Trimmomatic: a flexible trimmer for Illumina sequence data. Bioinform 30, 2114–2120. https://doi.org/10.1093/bioinformatics/btu170.

Borowiec, M.L., 2016. AMAS: a fast tool for alignment manipulation and computing of summary statistics. PeerJ 4, e1660. https://doi.org/10.7717/peerj.1660.

Breinholt, J.W., Carey, S.B., Tiley, G.P., Davis, E.C., Endara, L., McDaniel, S.F., Neves, L. G., Sessa, E.B., von Konrat, M., Chantanaorrapint, S., Fawcett, S., Ickert-Bond, S.M., Labiak, P.H., Larraín, J., Lehnert, M., Lewis, L.R., Nagalingum, N.S., Patel, N., Rensing, S.A., Testo, W., Vasco, A., Villarreal, J.C., Williams, E.W., Burleigh, J.G., 2021. A target enrichment probe set for resolving the flagellate land plant tree of life. Appl. Plant Sci. 9, e11406. https://doi.org/10.1002/aps3.11406.

Brock, J.M.R., 2025. Effective dispersal of fern spore and the ecological relevance of zoochory. Biol. Rev. 100, 2116–2130. https://doi.org/10.1111/brv.70038.

Camacho, C., Coulouris, G., Avagyan, V., Ma, N., Papadopoulos, J., Bealer, K., Madden, T.L., 2009. BLAST+: architecture and applications. BMC Bioinform. 10, 421. https://doi.org/10.1186/1471-2105-10-421.
Capella-Gutiérrez, S., Silla-Martínez, J.M., Gabaldón, T., 2009. trimAl: a tool for automated alignment trimming in large-scale phylogenetic analyses. Bioinform 25, 1972–1973. https://doi.org/10.1093/bioinformatics/btp348.
Cárdenas, G.G., Halme, K.J., Tuomisto, H., 2007. Riqueza y Distribución Ecológica de Especies de Pteridofitas en la Zona del Río Yavarí-Mirín, Amazonía Peruana. Biotropica 39, 637–646. https://doi.org/10.1111/j.1744-7429.2007.00308.x.
Cárdenas, G.G., Lehtonen, S., Tuomisto, H., 2019. Taxonomy and evolutionary history of the neotropical fern genus Salpichlaena (Blechnaceae). Blumea 64, 1–22. https://doi.org/10.3767/blumea.2018.64.01.01.
Cárdenas, G.G., Tuomisto, H., Lehtonen, S., 2016. Newly discovered diversity in the tropical fern genus Metaxya based on morphology and molecular phylogenetic analyses. Kew Bull. 71, 1–27. https://doi.org/10.1007/s12225-016-9618-9.
Chen, Z.J., 2010. Molecular mechanisms of polyploidy and hybrid vigor. Trends Plant Sci. 15, 57–71. https://doi.org/10.1016/j.tplants.2009.12.003.
Dexter, K.G., Pennington, T.D., Cunningham, C.W., 2010. Using DNA to assess errors in tropical tree identifications: how often are ecologists wrong and when does it matter? Ecol. Monogr. 80, 267–286. https://doi.org/10.1890/09-0267.1.
Doyle, J.J., Doyle, J.L., 1987. A rapid DNA isolation procedure for small quantities of fresh leaf tissue. Phytochem. Bull. 19, 11–15.
Dubuisson, J.-Y., Hennequin, S., Douzery, E.J., Cranfill, R.B., Smith, A.R., Pryer, K.M., 2003. rbcL phylogeny of the fern genus Trichomanes (Hymenophyllaceae), with special reference to neotropical taxa. Int. J. Plant Sci. 164, 753–761.
Dubuisson, J.-Y., Péchon, T.L., Hennequin, S., Rouhan, G., Salino, A., Deblauwe, V., Droissart, V., Tuomisto, H., Lehtonen, S., Ebihara, A., 2022. New insights into the diversity, taxonomy and history of the fern genus Trichomanes (Hymenophyllaceae, Polypodiidae), with a focus on Africa and the western Indian Ocean. Bot. J. Linn. Soc. 198, 215–239. https://doi.org/10.1093/botlinnean/boab049.
Ebihara, A., Dubuisson, J.-Y., Iwatsuki, K., Hennequin, S., Ito, M., 2006. A taxonomic revision of hymenophyllaceae. Blumea 51, 221–280. https://doi.org/10.3767/000651906X622210.
Ebihara, A., Iwatsuki, K., Ito, M., Hennequin, S., Dubuisson, J.-Y., 2007. A global molecular phylogeny of the fern genus Trichomanes (Hymenophyllaceae) with special reference to stem anatomy. Bot. J. Linn. Soc. 155, 1–27. https://doi.org/10.1111/j.1095-8339.2007.00684.x.
Ewels, P., Magnusson, M., Lundin, S., Käller, M., 2016. MultiQC: summarize analysis results for multiple tools and samples in a single report. Bioinform 32, 3047–3048. https://doi.org/10.1093/bioinformatics/btw354.
Fitzpatrick, B.M., 2012. Estimating ancestry and heterozygosity of hybrids using molecular markers. BMC Evol. Biol. 12, 131. https://doi.org/10.1186/1471-2148-12-131.
Frederiksen, L.K., Eiserhardt, W.L., Tuomisto, H., 2025. Speciation, dispersal and the build-up of fern diversity in the American tropics. Ecography 2025, e08170. https://doi.org/10.1002/ecog.08170.
Freeman, B.G., Pennell, M.W., 2021. The latitudinal taxonomy gradient. Trends Ecol. Evol. 36, 778–786. https://doi.org/10.1016/j.tree.2021.05.003.
Fridman, E., 2015. Consequences of hybridization and heterozygosity on plant vigor and phenotypic stability. Plant Sci. 232, 35–40. https://doi.org/10.1016/j.plantsci.2014.11.014.
Funk, W.C., Caminer, M., Ron, S.R., 2012. High levels of cryptic species diversity uncovered in Amazonian frogs. Proc. R. Soc. B 279, 1806–1814. https://doi.org/10.1098/rspb.2011.1653.
Goldenberg, R., Almeda, F., Caddah, M.K., Martins, A.B., Meirelles, J., Michelangeli, F. A., Weiss, M., 2013. Nomenclator botanicus for the neotropical genus *Miconia* (Melastomataceae: Miconieae). Phytotaxa 106, 1–171. https://doi.org/10.11646/phytotaxa.106.1.1.
González-Orozco, C.E., Parra-Quijano, M., 2023. Comparing species and evolutionary diversity metrics to inform conservation. Divers. Distrib. 29, 224–231. https://doi.org/10.1111/ddi.13660.
Hale, H., Gardner, E.M., Viruel, J., Pokorny, L., Johnson, M.G., 2020. Strategies for reducing per-sample costs in target capture sequencing for phylogenomics and population genomics in plants. Appl. Plant Sci. 8. https://doi.org/10.1002/aps3.11337.
Hassler, M., 2026. World Ferns. Synonymic Checklist and Distribution of Ferns and Lycophytes of the World. Version 26.05; last update May 20th, 2026 [WWW Document]. URL https://www.worldplants.de/ferns/. (accessed 21.05.26).
Hending, D., 2025. Cryptic species conservation: a review. Biol. Rev. 100, 258–274. https://doi.org/10.1111/brv.13139.
Hoang, D.T., Chernomor, O., von Haeseler, A., Minh, B.Q., Vinh, L.S., 2018. UFBoot2: improving the ultrafast bootstrap approximation. Mol. Biol. Evol. 35, 518–522. https://doi.org/10.1093/molbev/msx281.
Janzen, D.H., Burns, J.M., Cong, Q., Hallwachs, W., Dapkey, T., Manjunath, R., Hajibabaei, M., Hebert, P.D.N., Grishin, N.V., 2017. Nuclear genomes distinguish cryptic species suggested by their DNA barcodes and ecology. PNAS 114, 8313–8318. https://doi.org/10.1073/pnas.1621504114.
Jin, J.-J., Yu, W.-B., Yang, J.-B., Song, Y., dePamphilis, C.W., Yi, T.-S., Li, D.-Z., 2020. GetOrganelle: a fast and versatile toolkit for accurate de novo assembly of organelle genomes. Genome Biol. 21, 241. https://doi.org/10.1186/s13059-020-02154-5.
Johnson, M.G., Gardner, E.M., Liu, Y., Medina, R., Goffinet, B., Shaw, A.J., Zerega, N.J. C., Wickett, N.J., 2016. HybPiper: extracting coding sequence and introns for phylogenetics from high-throughput sequencing reads using target enrichment. Appl. Plant Sci. 4, 1600016. https://doi.org/10.3732/apps.1600016.
Kalyaanamoorthy, S., Minh, B.Q., Wong, T.K.F., von Haeseler, A., Jermiin, L.S., 2017. ModelFinder: fast model selection for accurate phylogenetic estimates. Nat. Methods 14, 587–589. https://doi.org/10.1038/nmeth.4285.
Kates, H.R., Johnson, M.G., Gardner, E.M., Zerega, N.J., Wickett, N.J., 2018. Allele phasing has minimal impact on phylogenetic reconstruction from targeted nuclear gene sequences in a case study of Artocarpus. Am. J. Bot. 105, 404–416. https://doi.org/10.1002/ajb2.1068.
Katoh, K., Standley, D.M., 2013. MAFFT multiple sequence alignment software version 7: improvements in performance and usability. Mol. Biol. Evol. 30, 772–780. https://doi.org/10.1093/molbev/mst010.
Keskiniva, V., Lehtonen, S., Testo, W., GoFlag Consortium, Tuomisto, H., 2025. Rampant hybridization in an old tropical fern genus (Danaea, Marattiaceae). Taxon 74, 536–552. https://doi.org/10.1002/tax.13315.
Keskiniva, V., Tuomisto, H., Lehtonen, S., 2024. Danaea (Marattiaceae) keeps diversifying, part 2: phylogeny and identification key for 81 taxa. Willdenowia 53, 229–255. https://doi.org/10.3372/wi.53.53304.
Leempoel, K., Bailey, P.C., 2025. Chloroplast Tree Of Life Pipeline. cpDNA.
Lehtonen, S., 2018. The complete plastid genome sequence of *Trichomanes trollii* (Hymenophyllaceae). Nord. J. Bot. 36. https://doi.org/10.1111/njb.02072.
Lehtonen, S., 2011. Towards resolving the complete fern tree of life. PLoS One 6, e24851. https://doi.org/10.1371/journal.pone.0024851.
Lehtonen, S., Muscarella, R., Moulatlet, G., Balslev, H., Tuomisto, H., 2021. Edaphic heterogeneity and the evolutionary trajectory of Amazonian plant communities. Ecol. Evol. 11, 17672–17685. https://doi.org/10.1002/ece3.8477.
Lellinger, D.B., 1994. Trichomanes polypodioides and its allies. Am. Fern J. 84, 1–4. https://doi.org/10.2307/1547550.
Lellinger, D.B., Windisch, P.G., 1994. *Trichomanes crispum* L. (Pteridophyta, Hymenophyllaceae) and allied species. Am. Fern J. 84, 10. https://doi.org/10.2307/1547553.
Li, H., Durbin, R., 2009. Fast and accurate short read alignment with Burrows-Wheeler transform. Bioinform 25, 1754–1760. https://doi.org/10.1093/bioinformatics/btp324.
Mace, G.M., 2004. The role of taxonomy in species conservation. Philos. Trans. R. Soc. Lond. B 359, 711–719. https://doi.org/10.1098/rstb.2003.1454.
Maltsev, Y., Erst, A., 2023. Recent advances in the integrative taxonomy of plants. Plants 12, 4097. https://doi.org/10.3390/plants12244097.
Manton, I., 1950. Problems of Cytology and Evolution in the Pteridophyta. Camb. Univ. Press. Doi:10.5962/bhl.title.4667.
Minh, B.Q., Schmidt, H.A., Chernomor, O., Schrempf, D., Woodhams, M.D., von Haeseler, A., Lanfear, R., 2020. IQ-TREE 2: new models and efficient methods for phylogenetic inference in the genomic era. Mol. Biol. Evol. 37, 1530–1534. https://doi.org/10.1093/molbev/msaa015.
Nauheimer, L., Weigner, N., Joyce, E., Crayn, D., Clarke, C., Nargar, K., 2021. HybPhaser: a workflow for the detection and phasing of hybrids in target capture data sets. Appl. Plant Sci. 9. https://doi.org/10.1002/aps3.11441.
Nicholls, J.A., Pennington, R.T., Koenen, E.J.M., Hughes, C.E., Hearn, J., Bunnefeld, L., Dexter, K.G., Stone, G.N., Kidner, C.A., 2015. Using targeted enrichment of nuclear genes to increase phylogenetic resolution in the neotropical rain forest genus Inga (Leguminosae: Mimosoideae). Front. Plant Sci. 6. https://doi.org/10.3389/fpls.2015.00710.
Nitta, J.H., Schuettpelz, E., Ramírez-Barahona, S., Iwasaki, W., 2022. An open and continuously updated fern tree of life. Front. Plant Sci. 13, 909768. https://doi.org/10.3389/fpls.2022.909768.
Ottenburghs, J., 2020. Ghost introgression: spooky gene flow in the distant past. Bioessays 42, 2000012. https://doi.org/10.1002/bies.202000012.
Paris, C.A., Wagner, F.S., Wagner, W.H., 1989. Cryptic species, species delimitation, and taxonomic practice in the homosporous ferns. Am. Fern J. 79, 46–54. https://doi.org/10.2307/1547159.
Pelosi, J.A., Zumwalde, B.A., Testo, W.L., Kim, E.H., Burleigh, J.G., Sessa, E.B., 2024. All tangled up: unraveling phylogenetics and reticulate evolution in the vining ferns, *Lygodium* (Schizaeales). Am. J. Bot. 111, e16389. https://doi.org/10.1002/ajb2.16389.
Pérez-Escobar, O.A., Gottschling, M., Chomicki, G., Condamine, F.L., Klitgård, B.B., Pansarin, E., Gerlach, G., 2017. Andean mountain building did not preclude dispersal of lowland epiphytic orchids in the neotropics. Sci. Rep. 7, 4919. https://doi.org/10.1038/s41598-017-04261-z.
Perrie, L., Brownsey, P., 2007. Molecular evidence for long-distance dispersal in the New Zealand pteridophyte flora. J. Biogeogr. 34, 2028–2038. https://doi.org/10.1111/j.1365-2699.2007.01748.x.
Rojas, M., 1992. The species problem and conservation: what are we protecting? Conserv. Biol. 6, 170–178. https://doi.org/10.1046/j.1523-1739.1992.620170.x.
Ross, H.A., 2014. The incidence of species-level paraphyly in animals: a re-assessment. Mol. Phylogenet. Evol. 76, 10–17. https://doi.org/10.1016/j.ympev.2014.02.021.
Rothfels, C.J., Johnson, A.K., Hovenkamp, P.H., Swofford, D.L., Roskam, H.C., Fraser-Jenkins, C.R., Windham, M.D., Pryer, K.M., 2015. Natural hybridization between genera that diverged from each other approximately 60 million years ago. Am. Nat. 185, 433–442. https://doi.org/10.1086/679662.
Ruokolainen, K., Tuomisto, H., Vormisto, J., Pitman, N., 2002. Two biases in estimating range sizes of Amazonian plant species. J. Trop. Ecol. 18, 935–942. https://doi.org/10.1017/S0266467402002614.
Salovaara, K.J., Cárdenas, G.G., Tuomisto, H., 2004. Forest classification in an Amazonian rainforest landscape using pteridophytes as indicator species. Ecography 27, 689–700. https://doi.org/10.1111/j.0906-7590.2004.03958.x/full.
Shee, Z.Q., Frodin, D.G., Cámara-Leret, R., Pokorny, L., 2020. Reconstructing the complex evolutionary history of the papuasian schefflera radiation through herbariomics. Front. Plant Sci. 11. https://doi.org/10.3389/fpls.2020.00258.

Sigel, E.M., 2016. Genetic and genomic aspects of hybridization in ferns. J. Syst. Evol. 54, 638–655. https://doi.org/10.1111/jse.12226.
Soltis, P.S., Soltis, D.E., 2009. The role of hybridization in plant speciation. Annu. Rev. Plant Biol. 60, 561–588. https://doi.org/10.1146/annurev.arplant.043008.092039.
Testo, W., 2023. wtesto/GoFlagHybPipeline: Zenodo version. Doi:10.5281/ZENODO.7832165.
Tryon, R., 1970. Development and evolution of fern floras of oceanic islands. Biotropica 2, 76. https://doi.org/10.2307/2989765.
Tseng, Y.-H., Kuo, L.-Y., Borokini, I., Fawcett, S., 2024. The role of deep hybridization in fern speciation: examples from the Thelypteridaceae. Am. J. Bot. 111, e16388. https://doi.org/10.1002/ajb2.16388.
Tumescheit, C., Firth, A.E., Brown, K., 2022. CIAlign: a highly customisable command line tool to clean, interpret and visualise multiple sequence alignments. PeerJ 10, e12983.
Tuomisto, H., Poulsen, A.D., 1996. Influence of edaphic specialization on pteridophyte distribution in neotropical rain forests. J. Biogeogr. 23, 283–293. https://doi.org/10.1046/j.1365-2699.1996.00044.x.
Tuomisto, H., Ruokolainen, K., Poulsen, A.D., Moran, R.C., Quintana, C., Cañas, G., Celi, J., 2002. Distribution and diversity of pteridophytes and melastomataceae along edaphic gradients in Yasuní National Park, Ecuadorian Amazonia. Biotropica 34, 516–533. https://doi.org/10.1111/j.1744-7429.2002.tb00571.x.
Van Doninck, J., Jones, M.M., Zuquim, G., Ruokolainen, K., Moulatlet, G.M., Sirén, A., Cárdenas, G., Lehtonen, S., Tuomisto, H., 2020. Multispectral canopy reflectance improves spatial distribution models of Amazonian understory species. Ecography 43, 128–137. https://doi.org/10.1111/ecog.04729.
Walker, T.G., 1985. Cytotaxonomic studies of the ferns of Trinidad 2. The cytology and taxonomic implications. Bulletin of the British Museum (Natural History), Botany 13, 149–249.
Walton, A., Aylward, A., Thomas, M.G., Rutherford, A., 2025. The history of the panmictic population concept and its legacy in contemporary population genetics. Ann. Hum. Genet. 89, 274–284. https://doi.org/10.1111/ahg.70015.
Wang, J., Dong, S., Yang, L., Harris, A., Schneider, H., Kang, M., 2020. Allopolyploid speciation accompanied by gene flow in a tree fern. Mol. Biol. Evol. 37, 2487–2502. https://doi.org/10.1093/molbev/msaa097.
Weismann, A., 1883. On Heredity, in: Essays Upon Heredity and Kindred Biological Problems. Clarendon Press, pp. 67–106.
Wolf, P.G., Schneider, H., Ranker, T.A., 2001. Geographic distributions of homosporous ferns: does dispersal obscure evidence of vicariance?: Dispersal and vicariance in ferns. J. Biogeogr. 28, 263–270. https://doi.org/10.1046/j.1365-2699.2001.00531.x.
Yasuda, N., Taquet, C., Nagai, S., Fortes, M., Fan, T.-Y., Harii, S., Yoshida, T., Sito, Y., Nadaoka, K., 2015. Genetic diversity, paraphyly and incomplete lineage sorting of mtDNA, ITS2 and microsatellite flanking region in closely related Heliopora species (Octocorallia). Mol. Phylogenet. Evol. 93, 161–171. https://doi.org/10.1016/j.ympev.2015.07.009.
Yi, H., Dong, S., Yang, L., Wang, J., Kidner, C., Kang, M., 2023. Genome-wide data reveal cryptic diversity and hybridization in a group of tree ferns. Mol. Phylogenet. Evol. 184, 107801. https://doi.org/10.1016/j.ympev.2023.107801.
Zhang, C., Mirarab, S., 2022. Weighting by gene tree uncertainty improves accuracy of quartet-based species trees. Mol. Biol. Evol. 39, msac215. https://doi.org/10.1093/molbev/msac215.
Zhang, C., Zhao, Y., Braun, E.L., Mirarab, S., 2021. TAPER: Pinpointing errors in multiple sequence alignments despite varying rates of evolution. Methods Ecol. Evol. 12, 2145–2158. https://doi.org/10.1111/2041-210X.13696.